

## A MICROPROBE STUDY OF ANTIGORITE AND SOME SERPENTINE PSEUDOMORPHS

MICHAEL A. DUNGAN

Department of Geological Sciences, Southern Methodist University, Dallas, Texas 75275, U.S.A.

### ABSTRACT

Microprobe analyses of serpentine pseudomorphs after olivine, orthopyroxene and clinopyroxene demonstrate partial inheritance of compositional characteristics from the parent phases. Bastites have higher chromium and aluminum contents than mesh-textured serpentine. Qualitative estimates of elemental mobility during serpentinization are  $Fe \gg Al > Cr$ . The observed persistence of lizardite bastites in progressively metamorphosed serpentinites suggests a compositional control. The presence of aluminum in solid solution may increase the thermal stability of lizardite with respect to antigorite or to partly dehydrated assemblages. The microprobe analyses confirm the compositional differences between pseudomorphic serpentines (lizardite and chrysotile) and antigorite that are predicted by their slightly different structural formulae: antigorites have lower  $H_2O$ , lower octahedral occupancies and relatively high  $SiO_2$ .

### SOMMAIRE

D'après les analyses à la microsonde, les serpentines pseudomorphes d'olivine, orthopyroxène ou clinopyroxène héritent certaines caractéristiques de la composition originelle. Les bastites contiennent plus de Cr et d'Al que les serpentines à texture réticulée. Pendant la serpentinisation, la mobilité relative des éléments est représentée, à l'estime, par le schéma  $Fe \gg Al > Cr$ . La persistance de la bastite à lizardite au cours du métamorphisme progressif des serpentinites témoigne de l'influence du facteur composition. La présence d'aluminium en solution solide dans la lizardite pourrait accroître la stabilité thermique par rapport à l'antigorite ou à des assemblages partiellement déshydratés. On confirme à la microsonde des divergences de composition entre les espèces pseudomorphes (lizardite et chrysotile) et l'antigorite, divergences que font prévoir des formules structurales légèrement différentes: les antigorites contiennent moins d'eau, plus de lacunes en position octaédrique et une teneur en  $SiO_2$  relativement élevée.

(Traduit par la Rédaction)

### INTRODUCTION

The objective of this study is to analyze with the electron microprobe some mineralogical and textural varieties of rock-forming serpen-

tine. There are two major petrological types of serpentinite, each distinct in its mineralogy, texture and petrogenesis (Coleman 1971). The most abundant type consists of serpentinites formed by the hydration of peridotites, referred to here as *pseudomorphic serpentinites*. Their serpentine mineralogy is lizardite plus minor chrysotile, and they are characterized by textures that are strictly indicative of retrograde replacement of olivine, orthopyroxene, clinopyroxene and, more rarely, tremolite, talc and anthophyllite. *Antigorite serpentinites* are formed largely by recrystallization of pseudomorphic serpentinites during progressive metamorphism (Coleman 1971, Wicks & Whittaker 1977). These relatively coarse-grained rocks consist of aggregates of interlocking antigorite blades. If thermal upgrading proceeds to sufficiently elevated temperatures (*i.e.* 400–600°C), antigorite serpentinites may become further reconstituted to forsterite-antigorite rocks or completely dehydrated to form secondary peridotites (Peters 1968, Matthes 1971, Vance & Dungan 1977).

Microprobe analyses in conjunction with mineralogical and textural evidence indicate that different factors control the compositions of pseudomorphic serpentines and antigorite. Contrasts in the nature of the equilibria associated with the two types of serpentinite are evaluated in relation to the compositions of the phases analyzed. The persistence in antigorite serpentinites of lizardite bastites after orthopyroxene and clinopyroxene is also discussed in the light of compositional differences between mesh-textured serpentine and the bastites.

### PREVIOUS WORK

Faust & Fahey (1962), Page (1967) and Whittaker & Wicks (1970) have attempted to define the compositional characteristics of the serpentine minerals through an evaluation of published analyses. Faust & Fahey (1962) compiled the serpentine analyses available at that time. Page (1968) added new data (Page & Coleman 1967) but discarded many old, questionable analyses from the Faust & Fahey list-

ing. Page also presented a discussion of the compositional differences among the serpentine minerals based on this new list. Whittaker & Wicks (1970) limited the group even further by eliminating all analyses that, in their opinion, were not unambiguously identified or that may have included minor amounts of additional phases. Trommsdorff & Evans (1972) and Frost (1975) included microprobe analyses of antigorite and coexisting phases in partly dehydrated, progressively metamorphosed serpentinites.

Geological studies of the Sultan Complex and the associated Darrington peridotites were reported by Vance (1972), Dungan & Vance (1972), Johnson *et al.* (1977), Dungan (1974, 1977, 1979), Vance & Dungan (1977) and Vance *et al.* (1980). The majority of serpentine samples from which analytical data have been collected are from the Sultan Complex. However, additional samples from several west-coast ultramafic bodies have also been analyzed. The representative analyses tabulated here are abstracted from a larger body of data included in Dungan (1974); these have been used in the discussion and in the preparation of figures. Complete tables of serpentine analyses are available on request.

#### ANALYTICAL TECHNIQUES

##### *Identification of the serpentine minerals*

Antigorite is the most easily identified serpentine mineral, by both its habit and its comparatively distinctive X-ray-diffraction pattern (Whittaker & Zussman 1956, Page & Coleman 1967). Antigorite in monomineralic serpentinites forms a flame-like or radiating bladed texture. Where it is in textural equilibrium with olivine it generally occurs in a lepidoblastic fabric of anhedral blades intergrown with granular olivine. This textural style is, in contrast, atypical of serpentine-olivine relationships in pseudomorphic serpentinites. The contrast in textural relationships between coarse-grained antigorite and strictly pseudomorphic serpentine provides an adequate criterion for distinguishing the two types. Whole-rock powders of antigorite serpentinites lacking olivine were analyzed by X-ray diffraction and gave patterns that indicate the absence of other serpentine minerals. Intimate intergrowths between antigorite and olivine prevented the separation of pure antigorite by heavy-liquid techniques. However, the texture of antigorite-olivine intergrowths is so distinct from pseudomorphic textures that misidentification is improbable.

Secondary lizardite or six-layer serpentine that has replaced pseudomorphic serpentine superficially may resemble antigorite: both can occur in radiating aggregates. Several serpentinites in the Sultan Complex apparently contain secondary serpentine that is not antigorite. These occurrences were tentatively identified on the basis of petrography and microprobe data, but chemical analyses are not reported.

Mineral identification of the various textural components of pseudomorphic serpentinites is far more difficult than in antigorite serpentinites. The textural complexity of the Sultan Complex pseudomorphic serpentinites eliminated whole-rock X-ray diffraction as a viable method for establishing the mineralogy of individual textural types except in a few samples. The results of earlier mineralogical determinations of serpentine textures were relied upon for providing mineral identification of serpentine pseudomorphs (Wicks 1969, Wicks & Whittaker 1977, Wicks & Zussman 1975). The results of these studies demonstrate that lizardite is the dominant mineral in serpentine pseudomorphs, particularly in bastites. Mesh-textured serpentine after olivine may be composed entirely of lizardite or intergrowths of lizardite and chrysotile ( $\pm$  brucite) with lizardite predominating. On the basis of these results, microprobe analyses of Sultan Complex bastites are presumed to be lizardite. It is inferred that microprobe analyses of mesh-textured serpentine probably reflect lizardite compositions, but it is acknowledged that this has not been specifically established and that they may also be bimineralic. However, there is some value in comparing antigorite analyses with analyses of lizardite or lizardite plus chrysotile, since there are differences in the structural formulae between (1) antigorite and (2) lizardite or chrysotile. Where this comparison is made, lizardite and chrysotile have been grouped together as pseudomorphic serpentines.

##### *Microprobe-analysis techniques*

Microprobe analyses were performed by standard techniques at 15 kV and 0.5 to 1.5 mA on an ARL EMX-SM five-channel microprobe. Iron, nickel, manganese, aluminum and chromium were standardized against natural olivines, a synthetic aluminous enstatite and a natural chromite, respectively. A natural antigorite supplied by R. G. Coleman (94 NA 62, Page & Coleman 1967) was used as a magnesium and silicon standard. This antigorite was reanalyzed using natural olivines for Si, Mg and Fe and a synthetic Al-enstatite for aluminum with the

following results: SiO<sub>2</sub> 44.5, Al<sub>2</sub>O<sub>3</sub> 0.64, MgO 39.7 and FeO 3.1 (all values in wt. % oxide). The MgO and FeO values are in near-perfect agreement with the published gravimetric analysis (Fe<sub>2</sub>O<sub>3</sub> and FeO recalculated to FeO). However, the SiO<sub>2</sub> value is substantially higher (44.5 versus 43.1%) and the Al<sub>2</sub>O<sub>3</sub> value is lower (0.64 versus 1.3%). This suggests that results of the gravimetric analysis suffer from Si-Al interference.

All microprobe data were corrected for background, dead-time, absorption, fluorescence and mean atomic number. Matrix corrections were also made for the presence of H<sub>2</sub>O; its concentration was estimated by difference from total anhydrous oxides.

Serpentine pseudomorphs and, to a lesser extent, antigorite, are inhomogeneous on a very fine scale. This variation is sporadic and does not reflect any systematic zoning pattern, with the possible exception of mesh-textured serpentine, which in some cases shows very minor but regular variation in Mg/Fe between different textural components. Aluminum in Al-rich bastites is variable. The analyses of antigorite and serpentine pseudomorphs reported here are averages of ten or more readings, with extreme values edited prior to data reduction. Data were collected from one to three pseudomorphs *per* thin section, and good agreement among them was generally observed. Representative analyses of antigorite and mesh-textured opx-bastite and cpx-bastite serpentines are reported in Tables 1, 2, 3 and 4.

## CRYSTAL CHEMISTRY OF SERPENTINES

### Crystallographic and structural formulae

Coleman (1971) noted that the structural diversity of the serpentine minerals is a product of the mismatch between the lateral dimensions of the Si-occupied tetrahedral sheet and the Mg-occupied octahedral sheet. The mismatch is overcome through various combinations of curvature, structural distortions and variations in the lateral dimensions of the sheets by substitutions of various cations for Mg and Si. Detailed discussions of serpentine crystallography can be found in Kunze (1961), Radoslovich (1963), Chernosky (1975), Wicks & Whittaker (1975) and Wicks & Zussman (1975).

Chrysotile, which apparently accepts only minor substitutions in its octahedral and tetrahedral sites, accommodates the mismatch through curvature to produce a cylindrical structure. Mg-lizardite has a platy structure that requires considerable lateral stretching of

TABLE 1. MICROPROBE ANALYSES OF ANTIGORITES

Sample	16	1	89	63	1320	81	242	5013	54.1
SiO <sub>2</sub>	44.9	44.9	43.9	45.0	45.4	43.9	43.5	42.1	43.4
Al <sub>2</sub> O <sub>3</sub>	0.31	0.65	1.9	0.62	0.34	0.68	1.3	2.5	0.90
Cr <sub>2</sub> O <sub>3</sub>	0.06	0.03	0.01	0.12	0.10	0.01	0.13	0.76	0.18
MgO	40.4	39.1	39.3	39.4	39.8	38.7	36.8	37.5	39.9
FeO*	1.9	3.5	3.9	3.1	2.7	4.6	6.2	4.7	3.4
MnO	0.01	0.03	0.05	0.04	0.03	0.05	0.10	0.05	0.04
NiO	0.08	0.06	0.04	0.05	0.26	0.05	0.16	0.24	0.17
Total	87.7	88.3	89.1	88.3	88.6	88.0	88.2	87.9	88.0
H <sub>2</sub> O**	12.3	11.7	10.9	11.7	11.4	12.0	11.8	12.1	12.0
***Number of ions on the basis of 13.626 oxygens									
Si	4.019	4.019	3.910	4.018	4.036	3.969	3.962	3.834	3.914
Al	0.033	0.069	0.194	0.060	0.036	0.073	0.137	0.272	0.096
Cr	0.004	0.002	0.001	0.008	0.007	0.001	0.009	0.055	0.013
Mg	5.387	5.216	5.221	5.241	5.271	5.222	4.993	5.092	5.364
Fe	0.139	0.259	0.288	0.231	0.197	0.368	0.470	0.354	0.256
Mn	0.001	0.002	0.004	0.003	0.002	0.004	0.008	0.004	0.003
Ni	0.006	0.004	0.003	0.004	0.019	0.004	0.012	0.010	0.012
ΣOct.	5.570	5.552	5.621	5.547	5.532	5.621	5.591	5.621	5.658
ΣCations	9.589	9.571	9.621	9.565	9.568	9.621	9.591	9.621	9.658

\*Total Fe as FeO. \*\*\*Calculated as anhydrous. \*\*Estimated by difference

Sample localities:

1, 63, 81 - Gordon Ridge, northern Sultan Complex, Wash.  
 1320 - Darrington peridotite, Washington. Collected by J. A. Vance  
 242 - Coast Range Ophiolite, California. Collected by H. I. Christensen  
 5013, 54.1 - Ultramafic bodies in Skagit Gneiss, Washington. Collected by P. Misch  
 16, 89 - Long Mountain, northern Sultan Complex, Washington

TABLE 2. MICROPROBE ANALYSES OF MESH-TEXTURED SERPENTINE

	114	80	113	29	109	221	27	222
SiO <sub>2</sub>	42.4	43.1	43.0	43.1	43.3	42.5	42.4	42.8
Al <sub>2</sub> O <sub>3</sub>	0.44	1.3	1.1	0.09	1.7	1.1	0.26	1.6
Cr <sub>2</sub> O <sub>3</sub>	0.01	0.02	0.02	0.01	0.06	0.01	0.04	0.01
MgO	41.0	38.9	40.1	41.9	37.7	41.0	41.2	39.5
FeO*	3.0	3.7	1.8	1.2	4.6	3.0	2.5	3.3
MnO	0.04	0.10	0.08	0.16	0.08	0.05	0.02	0.07
NiO	0.03	0.11	0.02	0.05	0.16	0.07	0.12	0.07
Total	86.9	87.2	86.1	86.5	87.4	87.7	86.5	87.4
H <sub>2</sub> O**	13.1	12.8	13.9	13.5	12.6	12.3	13.5	12.6
***Number of ions on the basis of 14.000 oxygens								
Si	3.979	4.028	4.029	4.022	4.045	3.947	3.984	3.993
Al	0.069	0.143	0.121	0.010	0.191	0.119	0.029	0.173
Cr	0.001	0.001	0.001	0.001	0.004	0.001	0.003	0.001
Mg	5.731	5.420	5.612	5.830	5.259	5.683	5.778	5.485
Fe	0.232	0.290	0.139	0.095	0.340	0.235	0.195	0.258
Mn	0.003	0.008	0.006	0.013	0.006	0.004	0.002	0.006
Ni	0.002	0.008	0.002	0.004	0.012	0.005	0.009	0.005
ΣOct.	5.997	5.870	5.881	5.953	5.812	5.994	6.000	5.921
ΣCations	9.997	9.898	9.910	9.975	9.857	9.994	10.000	9.921

\*Total Fe as FeO. \*\*\*Calculated as anhydrous. \*\*Estimated by difference

Sample localities: 29, 27 - northern Sultan Complex;  
 114, 80, 113, 109, 221, 222, 125, 220 - southern Sultan Complex.

the tetrahedral sheet and compression of the octahedral sheet, accommodated by rotation of bond angles to overcome the mismatch. Substitution of cations, particularly Al in the tetrahedral site and Cr<sup>3+</sup> and Fe<sup>3+</sup> in the octahedral site, also reduces the mismatch between sheets by changing their dimensions. Lizardite has a greater capacity to accept substitution than does chrysotile (Chernosky 1975). Despite this capacity, the Mg-end-member formula for both species is Mg<sub>6</sub>Si<sub>4</sub>O<sub>10</sub>(OH)<sub>8</sub>.

Kunze (1956, 1958, 1961) has shown that the antigorite structural formula differs from that of lizardite and chrysotile. Its accommodation to the misfit between the octahedral and tetrahedral sheets is accomplished by periodic

TABLE 3. MICROPROBE ANALYSES OF ORTHOPYROXENE BASTITES

Sample	80	113	129	242	104	1640	79	109	221	222	125	35	220
SiO <sub>2</sub>	42.3	42.5	41.1	42.9	42.3	41.3	40.4	41.0	41.4	42.8	41.2	41.8	43.2
Al <sub>2</sub> O <sub>3</sub>	2.5	1.5	3.6	2.4	2.4	1.9	4.7	2.9	4.7	2.3	2.5	3.4	2.4
Cr <sub>2</sub> O <sub>3</sub>	0.55	0.24	0.58	0.47	0.55	0.54	0.56	0.65	0.20	0.36	0.60	0.46	0.28
MgO	37.9	40.1	34.0	37.8	38.3	40.0	36.9	36.9	37.0	38.5	39.1	36.3	39.2
FeO*	3.9	1.9	7.9	3.9	3.8	3.4	3.6	4.8	4.2	3.4	2.8	5.4	2.9
MnO	0.12	0.11	0.18	0.12	0.05	0.04	0.08	0.08	0.08	0.06	0.08	0.12	0.10
NiO	0.07	0.20	0.08	0.20	0.06	0.18	0.06	0.13	0.02	0.01	0.10	0.11	—
Total	87.3	86.6	87.4	87.8	87.5	87.4	86.3	86.5	87.6	87.4	86.4	87.6	88.1
H <sub>2</sub> O***	12.7	13.4	12.6	12.2	12.5	12.6	13.7	13.5	13.4	13.6	13.6	13.4	11.9
Number of ions on the basis of 14,000 oxygens**													
Si	3.960	3.970	3.920	3.991	3.953	3.874	3.822	3.905	3.864	3.984	3.890	3.930	3.981
Al	0.274	0.166	0.409	0.265	0.269	0.211	0.525	0.322	0.516	0.257	0.276	0.372	0.265
Cr	0.041	0.018	0.044	0.035	0.041	0.040	0.042	0.049	0.015	0.026	0.045	0.034	0.020
Mg	5.292	5.580	4.834	5.241	5.327	5.595	5.208	5.238	5.141	5.341	5.503	5.087	5.382
Fe	0.307	0.146	0.626	0.303	0.293	0.263	0.287	0.379	0.328	0.261	0.222	0.426	0.221
Mn	0.010	0.009	0.015	0.009	0.004	0.003	0.006	0.006	0.006	0.005	0.006	0.010	0.008
Ni	0.005	0.015	0.006	0.015	0.005	0.014	0.005	0.010	0.002	0.001	0.008	0.008	—
Σ Oct.	5.889	5.904	5.853	5.859	5.892	6.000	5.895	5.909	5.872	5.872	5.950	5.867	5.877
Σ Cations	9.899	9.904	9.853	9.859	9.892	10.000	9.895	9.909	9.872	9.875	9.950	9.867	9.877

\*Total Fe as FeO. \*\*Calculated as anhydrous. \*\*\*Estimated by difference

#### Sample localities:

80, 113, 79, 109, 221, 222, 125 and 220—southern Sultan Complex;  
129, 104 and 35 Gordon Ridge, northern Sultan Complex;  
242 - Coast Range Ophiolite, California; collected by N. I. Christensen;  
1640 - Darrington peridotite; collected by J. A. Vance

inversions in curvature that produce an alternating-wave structure. The apical oxygens of the tetrahedral sheet point in opposite directions in each alternating section of the wave structure, so that the tetrahedral sheet is joined to the octahedral sheet above it in one half of the wave and the octahedral sheet below it in the next half of the wave. The octahedral sheet in each half-wave is joined to the octahedral sheet in the next half-wave by Mg bridges. The full-wave repeat distance defines the *a* superlattice parameter, found to vary from 16 to 110 Å (Zussman *et al.* 1957). Kunze (1961) suggested that preferred *a*-axis parameters should fall in the range of 25–52 Å, which agrees closely with the observed frequency of values (in the interval 35–45 Å) measured by Zussman *et al.* (1957). The alternating-wave structure produces deficiencies of Mg<sup>2+</sup> and OH<sup>-</sup> compared with the ideal serpentine formula. For the purpose of standardizing a number of oxygens for normalization of cation proportions, a structural formula of Mg<sub>5.626</sub>Si<sub>4</sub>O<sub>10</sub>(OH)<sub>7.353</sub> (*i.e.*, 13.626 oxygens/formula unit on an anhydrous basis) has been adopted. It must be emphasized that this formula has been chosen as a reasonable average and will not be accurate for all antigorites. Nonetheless, the

normalization of antigorite cations to 13.626 oxygens has yielded good results in the present study and is preferable to the use of 14,000 oxygens, as the latter inevitably results in excess Si+Al<sup>IV</sup>.

#### Chemical differences among the serpentine minerals related to contrasting structural formulae

Table 5 is a comparison of serpentine Mg-end-member compositions calculated on the basis of the lizardite-chrysotile formula and the 43.5 Å antigorite formula. The antigorite has greater SiO<sub>2</sub> and less H<sub>2</sub>O and MgO relative to lizardite and chrysotile. The microprobe analyses presented in Tables 1–4 indicate a very close correspondence between the natural compositions and predictions based on the structural formulae.

Figure 1 is a histogram of the totals of anhydrous oxides of serpentines analyzed by Dungan (1974). Water contents, estimated by difference, are 14.3 to 11.9% for pseudomorphic serpentines and 12.9 to 10.9% for antigorite. The average of the former is 12.8, which closely approximates the ideal value of 12.99 (Table 5). The average H<sub>2</sub>O content of the

TABLE 4. MICROPROBE ANALYSES OF CLINOPYROXENE BASTITES

Sample	68	62	114	80	113	104	79	109	125	81
SiO <sub>2</sub>	39.8	42.3	40.7	41.6	40.8	38.4	41.4	41.1	41.3	42.1
Al <sub>2</sub> O <sub>3</sub>	4.3	0.94	2.3	2.1	3.1	5.7	2.7	2.1	1.7	1.3
Cr <sub>2</sub> O <sub>3</sub>	0.53	0.55	0.51	0.90	0.50	1.05	0.73	0.81	0.65	0.50
MgO	37.9	40.0	40.3	39.3	38.9	37.6	38.2	38.7	39.7	9.2
FeO*	4.6	2.8	2.6	2.9	2.1	3.6	4.1	3.8	3.4	4.3
MnO	0.04	0.05	0.02	0.06	0.12	0.04	0.05	0.04	0.03	0.07
NiO	0.04	0.03	0.02	0.04	0.18	0.05	0.05	0.14	0.17	0.04
Total	87.2	86.7	86.5	86.9	85.7	86.4	87.2	86.7	87.0	7.5
H <sub>2</sub> O***	12.8	13.3	13.5	13.1	14.3	13.7	12.8	13.3	13.0	2.5
** Number of ions on the basis of 14.000 oxygens										
Si	3.759	3.976	3.840	3.904	3.866	3.652	3.895	3.889	3.895	3.951
Al	0.483	0.104	0.257	0.237	0.348	0.639	0.296	0.235	0.184	0.143
Cr	0.040	0.041	0.038	0.067	0.038	0.079	0.054	0.061	0.048	0.037
Mg	5.332	5.606	5.667	5.503	5.499	5.324	5.358	5.465	5.576	5.479
Fe	0.360	0.218	0.207	0.225	0.168	0.288	0.319	0.300	0.271	0.340
Mn	0.003	0.004	0.002	0.005	0.010	0.003	0.004	0.003	0.002	0.006
Ni	0.003	0.002	0.002	0.003	0.014	0.004	0.004	0.011	0.013	0.003
Σ Oct.	5.979	5.951	6.013	5.944	5.943	5.989	5.930	5.964	5.989	5.959
Σ Cations	9.979	9.951	10.013	9.944	9.943	9.989	9.930	9.964	9.989	9.959

\*Total Fe as FeO. \*\*Calculated as anhydrous. \*\*\*Estimated by difference

#### Sample localities:

68, 62, 104, 81 - northern Sultan Complex;  
114, 80, 113, 79, 109, 125 - southern Sultan Complex

antigorites analyzed in this study is 11.9%, which is lower than the calculated value (12.34). However, this may reflect in part some real variations in antigorite structural formulae and in Fe<sub>2</sub>O<sub>3</sub>/FeO, which would cause shifts in H<sub>2</sub>O content. There is good agreement between oxide totals for antigorite obtained in this study and microprobe analyses reported by Trommsdorff & Evans (1972) and Frost (1973). Although there are minor discrepancies between the microprobe analyses and the wet-chemical data assembled by Page (1967) and Whittaker & Wicks (1970), both sets of data are in substantial agreement with the prediction that antigorite should contain 0.7% less H<sub>2</sub>O than pseudomorphous serpentines.

The serpentine minerals are complex solid-solution series involving substitution of divalent and trivalent cations for Mg in the octahedral site and Al and perhaps Fe<sup>3+</sup> for Si in the tetrahedral site. Thus the Si and Mg contents of individual serpentines are a function of these solid-solution characteristics as well as their structural formulae. Chemical data in the present study demonstrate that substitution for Mg

and Si is more extensive in antigorite and lizardite than Page (1967) or Whittaker & Wicks (1970) recognized on the basis of the data available to them. Figure 2 summarizes the extent of substitution of Al + Cr and Fe, Mn and Ni in antigorites and pseudomorphous serpentinites analyzed by Dungan (1974). This diagram does not reflect strictly octahedral substitution since the normalization was based on total Al. Note the lower (Al + Cr) in mesh-textured serpentine.

The triangular plots used by Whittaker & Wicks (1970) to display graphically their compilation of analyses indicate that antigorite does indeed have higher SiO<sub>2</sub> than do lizardite and chrysotile. The microprobe data (Fig. 3) confirm that antigorites low in trivalent cations contain more SiO<sub>2</sub> than lizardite or chrysotile, as the differences in structural formulae predict. However, antigorites that contain substantial Al and Cr have lower silica values that overlap the lizardite-chrysotile range.

Figure 3 also compares the MgO values in antigorites and pseudomorphous serpentinites analyzed in Dungan (1974). The results of this

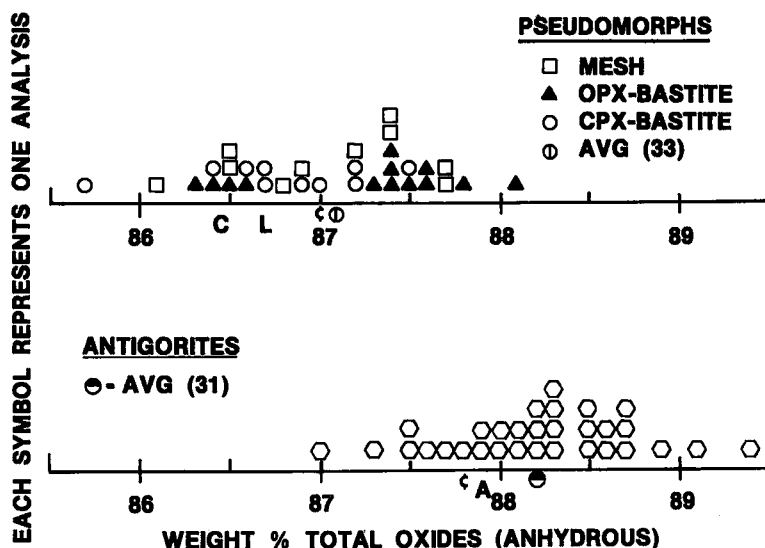


FIG. 1. Histogram of weight percent total oxides in serpentines. The higher oxide totals in antigorites reflect lower  $H_2O$  contents. Calculated anhydrous oxide totals for lizardite/chrysotile and antigorites at  $Fe^{3+} = 0$  are denoted by the symbol  $\phi$  below the scale. Figures for average total oxide taken from the compilation of analyses by Whittaker & Wicks (1970) are indicated by C = chrysotile, L = lizardite and A = antigorite.

TABLE 5. COMPARISON OF SERPENTINE STRUCTURAL FORMULAE

	Lizardite Chrysotile $Mg_6Si_4O_{10}(OH)_8$	Antigorite $Mg_{5.626}Si_4O_{10}(OH)_{7.353}$
SiO <sub>2</sub>	43.37	45.10
MgO	43.64	42.56
H <sub>2</sub> O	12.99	12.34
	100.00	100.00

study indicate that these two groups have highly variable MgO contents and that they overlap in MgO. However, antigorites and pseudomorphic serpentines may be distinguished on the basis of total octahedral occupancy. This method of comparison is valid only where cations are normalized to the appropriate number of oxygens. The average number of octahedral cations in 25 antigorites is 5.59 compared with 5.93 for 33 mesh-textured serpentines and bastites, most of which are presumed to be lizardite. Whereas the actual values are 0.7 and 1.3% low, respectively, the difference between the two averages is approximately equivalent to the amount predicted by the structural formulae. The calculated Si atoms/formula unit were found to be consistently higher in this study than stoichiometric values. This anomaly is reflected in the octahedral totals and  $Al^{IV}$  values, which

are too low to provide charge balance between the tetrahedral and octahedral sites. Such discrepancies could be the result of either octahedral vacancies or the presence of 10 Å talc-like structures interlayered with the 7 Å serpentine (Brindley & Hang 1973, Floran & Papike 1975).

#### THE CHEMISTRY OF SERPENTINE PSEUDOMORPHS

##### *Chemical differences among serpentine pseudomorphs*

Serpentine pseudomorphs after olivine, orthopyroxene and clinopyroxene are indistinguishable as groups on the basis of their Fe, Mg, Mn and Ni contents. However, there are significant differences with respect to Al and Cr, particularly in the comparison of mesh-textured serpentine with bastites. Mesh-textured pseudomorphs analyzed in this study contain only minor amounts of chromium (0.01–0.06 Cr<sub>2</sub>O<sub>3</sub>; one sample at 0.12, Table 2). The Cr<sub>2</sub>O<sub>3</sub> contents of opx-bastites range from 0.20 to 0.65% (Table 3), whereas cpx-bastites range from 0.44 to 1.2% (Table 4; the value of 1.2% pertains to a bastite that has recrystallized to antigorite. The highest Cr<sub>2</sub>O<sub>3</sub> content measured for a lizardite is 1.05%). The aluminum contents of mesh-textured serpentine are more

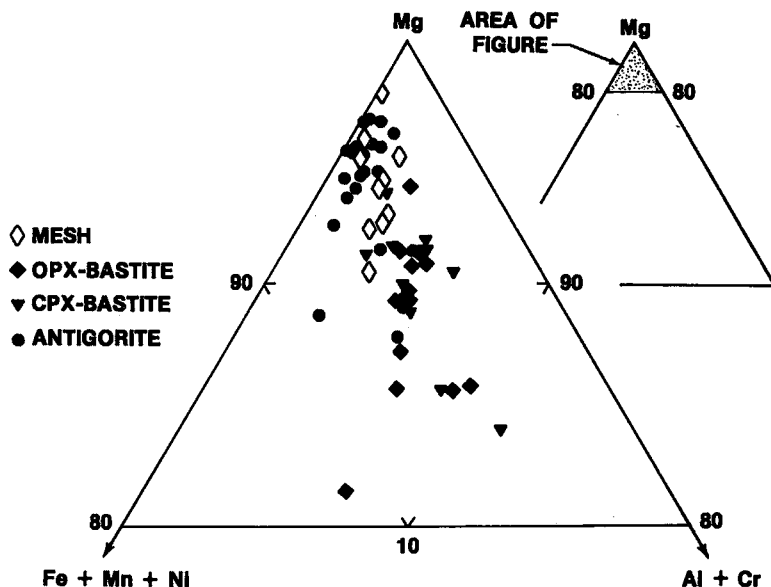


FIG. 2. Substitution in serpentine pseudomorphs and antigorite. Aluminum and chromium are grouped together, as they tend to vary sympathetically.

variable (0.09–1.7%  $\text{Al}_2\text{O}_3$ ) and overlap with low-Al bastites (Fig. 4).

#### Cation migration during serpentinization

Terrestrial forsterites contain less than 0.01%  $\text{Cr}_2\text{O}_3$  and  $\text{Al}_2\text{O}_3$  (Simkin & Smith 1970). Pyroxenes in ultramafic rocks invariably contain substantial Cr and Al. The pyroxenes in wehrlitic cumulates from the Sultan Complex contain up to 0.82%  $\text{Cr}_2\text{O}_3$  and 5.4%  $\text{Al}_2\text{O}_3$  (Dungan 1974). Clinopyroxene has a higher  $\text{Mg}/(\text{Mg} + \text{Fe})$  than coexisting olivine and orthopyroxene. These compositional contrasts among the parent silicates provide a standard for determining the extent to which cation migration occurs during serpentinization when the element-partitioning patterns between pairs of coexisting parent silicates and “coexisting” pseudomorphs are compared.

Chromium partitioning between coexisting orthopyroxene and clinopyroxene from the Sultan Complex cumulates favors the clinopyroxene ( $X\text{Cr}_{\text{opx}}/X\text{Cr}_{\text{cpx}} \approx 0.6$ ), and this relationship is grossly preserved by the respective groups of pseudomorphs (Fig. 5). More scatter is evident in the serpentine data, but the parent distribution is inherited in a general way by the bastites. The very low Cr contents of mesh-textured serpentine in adjacent pseudomorphs (Fig. 4) are further evidence that chromium

was relatively immobile during serpentinization of the Sultan Complex.

Aluminum partitioning between pairs of coexisting pyroxenes in the Sultan Complex defines a linear trend and slightly favors the

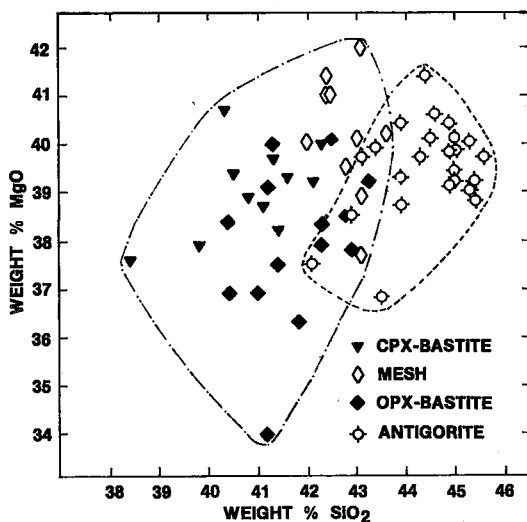


FIG. 3.  $\text{MgO}$  versus  $\text{SiO}_2$  in serpentines. Dashed lines encircle all antigorite analyses and all analyses of pseudomorphous serpentines. The maximum  $\text{SiO}_2$  values of the two groups correspond to the calculated values for the Mg end-members.

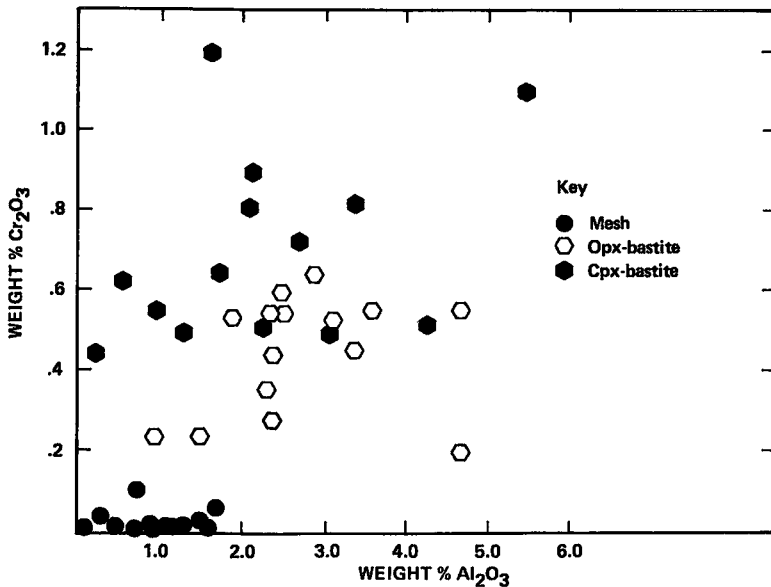


FIG. 4.  $\text{Cr}_2\text{O}_3$  versus  $\text{Al}_2\text{O}_3$  in pseudomorphous serpentines.

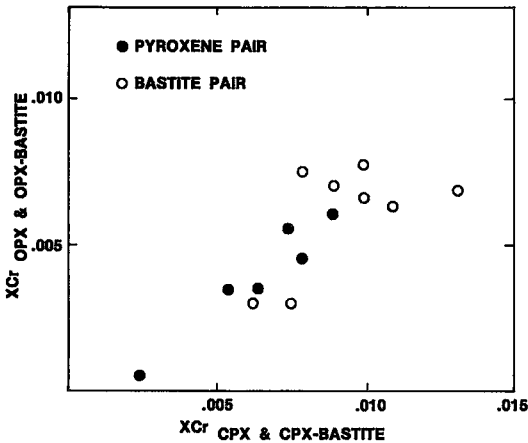


FIG. 5. Distribution of chromium between primary pyroxenes in the Sultan Complex and pairs of bastites after orthopyroxene and clinopyroxene. ( $X_{\text{Cr}} = \text{Cr}/\text{total octahedral cations}$ .)

clinopyroxenes at high Al values (Fig. 6). Below 3.5%  $\text{Al}_2\text{O}_3$  ( $\sim 0.19$  Al atoms per 6 oxygens) the distribution between pyroxenes appears to approach unity, *i.e.*,  $\text{Al}_{\text{opx}}/\text{Al}_{\text{cpx}} = 1.0$ . In Figure 6 a number of bastite pairs plot fairly close to the partitioning pattern defined by analyzed pyroxene pairs. However, some bastite pairs plot well off the line, and several others have anomalously low Al contents. The presence of up to 1.7%  $\text{Al}_2\text{O}_3$  ( $\sim 0.19$  Al atoms per 14 oxygens) in some mesh-textured serpentine demonstrates migration of Al during

serpentinization. The Al contents of mesh-textured serpentine increase slightly with increasing Al in coexisting bastites. This relationship may reflect Al migration in response to compositional gradients between mesh-textured and bastite serpentine.

A factor that greatly complicates the interpretation of the Al distribution in serpentinites, and to some extent that of Cr, is the concurrent alteration of accessory chromian spinel. Discussions of this phenomenon by Beeson & Jackson (1969), Ulmer (1974), Bliss & MacLean (1975) and Onyeagocha (1973) indicate that migration of Al and Cr does take place at least very locally and that extent of redistribution of these elements varies considerably at different localities.

Table 6 is a comparison of the ranges of  $\text{Mg}/(\text{Mg}+\text{Fe})$  in parent silicates and in their respective serpentine pseudomorphs. The higher ratio in serpentines is caused by the oxidation of iron (originally bound in parent silicates) during serpentinization with the attendant formation of magnetite. Brucite, which is also intergrown with serpentine formed in olivine-rich rocks, is more iron-rich than coexisting serpentine (Hostetler *et al.* 1966). Despite the low  $\text{Mg}/(\text{Mg}+\text{Fe})$  of olivine and orthopyroxene relative to clinopyroxene, the three types of pseudomorphs have roughly the same  $\text{Mg}/(\text{Mg}+\text{Fe})$ . The homogenization of iron and magnesium among the pseudomorphs is even more striking if the  $X_{\text{Fe}}$  values ( $X_{\text{Fe}} = \text{Fe}/\Sigma \text{ octahedral cations}$ ) of "coexisting" pairs

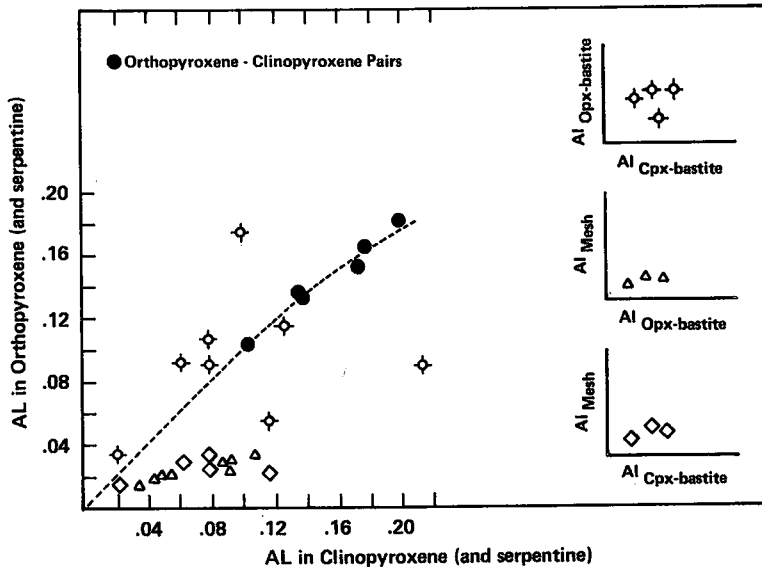


FIG. 6. Aluminum distribution between pyroxene pairs and serpentine pseudomorph pairs in the Sultan Complex. Al = Al atoms/formula unit. The three schematic plots on the right side of the diagram are keys to the axes and pairs of serpentine pseudomorph textural types to which the open symbols refer.

of pseudomorphs from single samples are evaluated. Figure 7 includes plots of the XFe in three combinations of pseudomorph pairs and the corresponding pairs of parent silicates. Although the serpentine data show significant scatter compared to the parent silicates, the coexisting pairs fairly closely approximate a 1:1 distribution.

#### THE NATURE OF SERPENTINE EQUILIBRIA

The contrasts in textural relations between antigorite and the metamorphic minerals with which it coexists on the one hand and the pseudomorph-parent silicate replacement-textures on the other are believed to reflect fundamental differences in the nature of the associated equilibria. Equilibrium metamorphic textures are presumed to indicate reversible reactions in that they are best interpreted as representing a state of dynamic chemical equilibrium. Metaserpentinities that exhibit such equilibrium textures are characterized by a progressive sequence of critical mineral assemblages that are related by reversible hydration-dehydration reactions (Evans & Trommsdorff 1970, Frost 1975). The textural relationships between parent silicates and their pseudomorphs do not suggest formation *via* reversible equilibria; rather, exclusively retrograde replacement seems

TABLE 6. Mg/(Mg + Fe) RATIOS

Parent Silicate	Mg/(Mg + Fe)	Pseudomorph	Mg/(Mg + Fe)
Olivine	0.86 - 0.81	Mesh	0.98 - 0.94
Orthopyroxene	0.86 - 0.81	Opx-Bastite	0.98 - 0.92*
Clinopyroxene	0.93 = 0.91	Cpx-Bastite	0.97 - 0.95

\*The Mg/(Mg + Fe) of opx-bastite in sample 129 = 0.86

to be indicated. The potentially metastable character of the reactions associated with the formation of bastites and mesh-textured serpentine are discussed elsewhere (Dungan 1977, 1979).

The Mg-Fe partitioning relationships between antigorite and coexisting olivine, talc, tremolite and diopside in metaserpentinities are defined by linear distributions indicative of the attainment of Fe-Mg exchange equilibrium (Trommsdorff & Evans 1972, Frost 1975, Vance & Dungan 1977). Microprobe analyses of partly serpentinized olivines demonstrate that their compositions do not change during pseudomorphic serpentinization. These observations seem to indicate that in pseudomorphic serpentinization, only the surfaces of the parent silicates participate in the reactions. If this premise is correct, the chemistry of the pseudomorphic serpentines must be a function of partial or

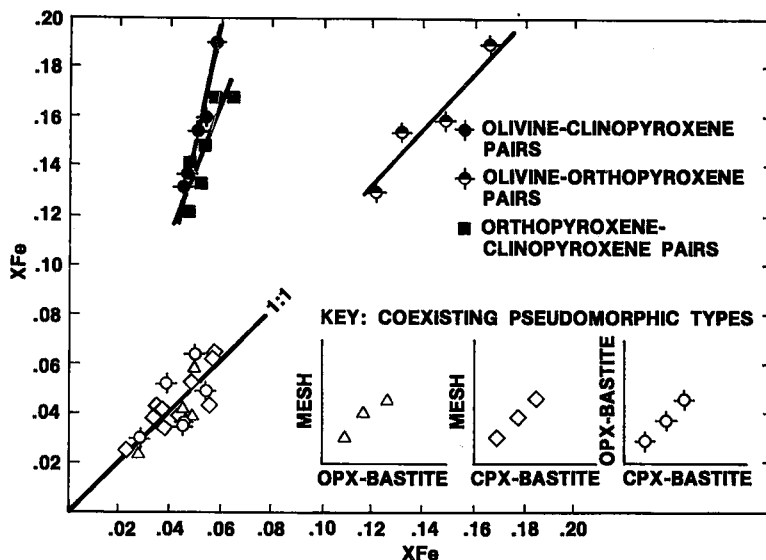


FIG. 7. A comparison of iron partitioning between pairs of coexisting ferromagnesian silicates and serpentine pseudomorphs in the Sultan Complex.  $X_{Fe} = Fe / \Sigma$  octahedral cations. The three schematic plots on the lower right of the diagram are keys to the axes and pairs of serpentine pseudomorph textural types to which the open symbols refer.

complete equilibration between serpentine and the aqueous serpentinizing fluid. Reactions of this type are compatible with the reaction models proposed by Brindley (1963) and Dungan (1977, 1979) and consistent with the low temperatures associated with pseudomorphic serpentinization and with observed elemental distribution patterns among serpentine pseudomorphs. Aluminum and chromium migrate very little because of their low solubilities in low-temperature aqueous solutions. Local migration of iron is demonstrated by the heterogeneous distribution of magnetite segregations in most pseudomorphic serpentinites and by the progressive change in magnetite grain-size and distribution with increasing serpentinization, as has been noted by Wicks & Whittaker (1977). The homogeneous distribution of iron among the pseudomorphs in the analyzed samples suggests that oxygen fugacity is buffered locally. Rucklidge & Patterson (1977) have suggested that a transient  $Fe_2(OH)_3Cl$  phase plays a role in mobilizing iron during serpentinization and is in part responsible for its distribution among serpentine pseudomorphs.

Several lines of evidence point to changes in oxygen fugacity with progressive serpentinization. Page (1967) and Eckstrand (1975) have recognized an increase in the production of magnetite in the advanced stages of serpentinization. In his detailed study of the Burro Moun-

tain peridotite, Page noted that slightly serpentinized rocks contain high-Fe serpentine with a relatively restricted compositional range. Serpentine in completely hydrated rocks have lower and more variable iron contents. Most of the pseudomorphic serpentines analyzed in the present study lack associated residual parent silicates, but the few that do contain relatively iron-rich serpentines. Most notable among these is the incipient bastite in sample 129. Some of the orthopyroxenes have been about 5% altered to bastite, and the lizardite formed has an anomalously low  $Mg/(Mg+Fe)$  of 0.86, which is identical to that of the parent phase. This apparently "primitive" pseudomorphic composition implies that the iron contents of serpentines tend to be progressively lowered by cation exchange with the fluid phase during or even after serpentinization.

#### COMMENTS ON THE STABILITY OF NATURAL AL-LIZARDITE

Vance & Dungan (1977) presented textural and chemical evidence that peridotites in the Sultan and Darrington areas are produced by deserpentinization during greenschist- to amphibolite-facies metamorphism. Many of these rocks have been recrystallized and partly dehydrated under static conditions, resulting in the preservation of relict serpentinite textures. The most prominent features are mag-

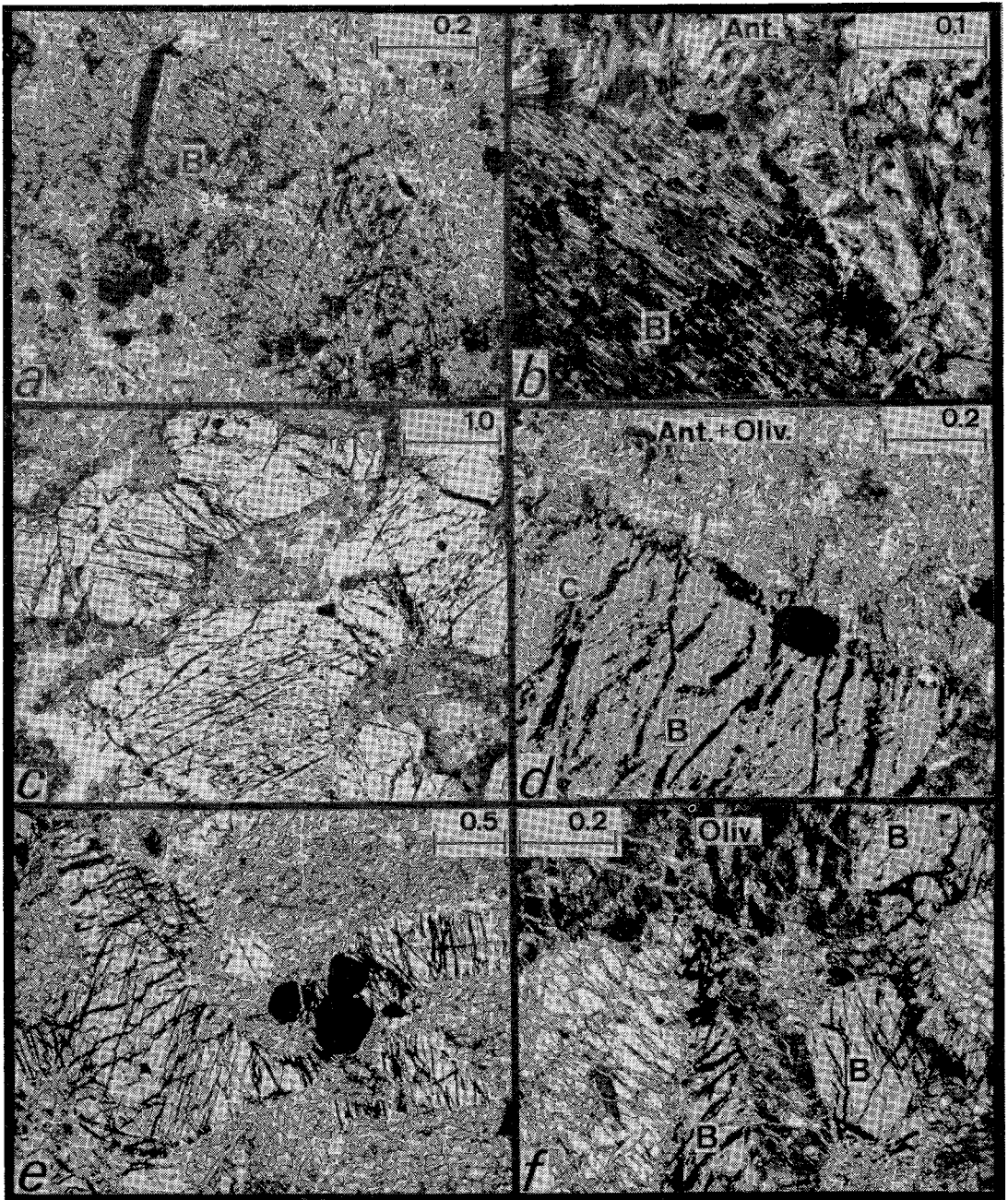


FIG. 8. Relict bastites (B) in metaserpentinites (scale in mm); all are shown in partially crossed polars. (a) Relict bastite in a matrix of bladed antigorite. (b) Detail of the contact near top of Fig. 8a. (c) Light-colored areas with linear segregations of magnetite are relict cpx-bastites in a matrix of fine-grained antigorite and newly formed olivine. (d) Detail of bastite-matrix boundary in Fig. 8c. C = carbonate. (e) Relict cpx-bastites in a matrix of newly formed olivine and minor antigorite. (f) Detail of Fig. 8e.

netite segregations formed during serpentinization and bastite pseudomorphs. Bastites in these rocks tend to persist as unrecrystallized lizard-

dite in contrast to adjacent mesh-textured pseudomorphs, which are recrystallized to antigorite or even dehydrated to form olivine.

This behavior has been examined in the light of compositional differences between the bastites and the matrix mesh-textured serpentine (Fig. 4). Theoretical considerations (Radoslovich 1963, Wicks & Whittaker 1975) and experimental studies (Chernosky 1975, Caruso & Chernosky 1979) indicate that substitution of various cations for Mg and Si in lizardite may have an effect on the stability of lizardite to other serpentine minerals and to its breakdown products.

#### *Petrography*

The recrystallization of mesh-textured pseudomorphs to radiating antigorite blades (interpenetrating texture of Wicks & Whittaker 1977) is the first reaction recorded in statically metamorphosed serpentinites in the Sultan Complex. With increasing metamorphic grade, antigorite and brucite react to form forsterite (Vance & Dungan 1977). Within this progressive sequence, bastites exhibit various degrees of recrystallization, but in the majority of examples observed in this study they are less modified by metamorphism than are the adjacent mesh-textured pseudomorphs.

The bastite shown in Figures 8a and 8b is typical of the persistent bastites found in an olivine-free metaserpentine. The matrix serpentine is an intergrowth of radiating antigorite blades. A few scattered blades of antigorite are present within the bastite, and a narrow veinlet of antigorite cuts the bastite near the centre of Figure 8a. In general, the boundary between the bastite and the antigorite is sharp and not penetrated by matrix antigorite (Fig. 8b).

A more advanced stage of recrystallization is shown in Figures 8c and 8d. The parent serpentine contains abundant bastites, apparently after clinopyroxene, and the relict cumulus textures are well preserved. In this sample, the mesh-textured serpentine matrix has been entirely recrystallized to antigorite and partly dehydrated to form fine-grained olivine. The boundaries between the bastites and the antigorite-olivine intergrowths are generally sharp, but antigorite blades do pierce the margins of the bastites in rare instances. Scattered antigorite blades do occur within the bastites but they also are rare. Olivine is completely absent in bastites, although partial replacement by dolomite has occurred.

In the third sample, illustrated in Figure 8e and 8f, deserpentinization of the matrix is nearly complete. The bastites are set in a matrix of granular, very magnesian olivine ( $F_{0.88}$ ) and minor antigorite. Minor retrograde lizardite rims

the individual olivine grains. As in the previous examples, the boundary between bastite and matrix is extremely sharp, and olivine is absent from the area of the bastite. Scattered needles of antigorite are present but most of the original lizardite remains unrecrystallized. The bastites are replaced by variable amounts of carbonate.

Many of the peridotites in the Darrington-Weden Creek area contain the assemblage forsterite + talc + tremolite, indicating final crystallization above the stability range of Al-poor antigorite. Relict bastites can be recognized in these rocks, but they are not as abundant as in the Sultan Complex. Although lizardite bastites do persist in rare examples, they are usually partly replaced by talc or talc + antigorite. Most of the bastites in the Darrington peridotites are completely converted to aggregates of talc + chlorite or talc + antigorite. Newly formed olivine is usually absent from the area of the bastites. In a minority of the samples observed in this study, bastites in metamorphosed serpentinites have recrystallized to antigorite along with their matrix. These samples exhibit petrographic evidence that deformation and shearing occurred prior to or during metamorphic recrystallization to antigorite.

#### *Implications for serpentine stability*

Roy & Roy (1954), Gillery (1959) and Shirozu & Momoi (1972) synthesized serpentines in the system  $MgO-Al_2O_3-SiO_2-H_2O$ ; in the experiments, the formation of platy serpentine was favored over chrysotile by increasing the Al content of the starting mix. Caruso & Chernosky (1979) repeated these experiments over a range of Al substitution and carefully monitored the results by determining the refractive indices and cell dimensions of the run products and by examining their habit with the electron microscope. Calculated cell parameters (Chernosky 1975) demonstrate that changes do occur as a result of aluminum substitution; these reflect shortening of the octahedral sheet and expansion of the tetrahedral layer. Caruso & Chernosky (1979) suggest that the relative stabilities of lizardite and antigorite are compositionally dependent and that the thermal stability of lizardite is substantially increased by aluminum solid-solution. The persistence of aluminous bastites in otherwise recrystallized serpentinites is presumed to be an example of this greater stability for lizardite. However, these occurrences do not allow one to discriminate between genuine stability and enhanced ability to persist metastably.

Substitution of trivalent cations in lizardite could minimize the  $\Delta G$  between stable antigorite and metastable lizardite, thereby decreasing the tendency for reaction. The presence of a few scattered needles of antigorite within otherwise unrecrystallized bastites indicates some tendency for replacement by antigorite. Metastable persistence is supported by the recrystallization of bastites in serpentinites that apparently have been deformed mildly during recrystallization. The improved kinetics associated with syntectonic recrystallization are probably adequate to overcome the sluggish reaction rates. The presence of chrysotile in mesh-textured serpentine and its absence in bastites may be significant in providing antigorite nucleation sites in the former.

The replacement of residual bastites by carbonate is generally far more advanced than the replacement of the matrix antigorite. Dietrich & Peters (1971) noted a similar relationship in the Oberhalbstein area, in which antigorite veins are free of carbonate in contrast to the matrix lizardite/chrysotile. The preferential replacement of lizardite by carbonate suggests that the antigorite may have been more stable under the T-X(CO<sub>2</sub>) conditions that prevailed during progressive metamorphism.

#### CONCLUSIONS

Microprobe analyses of antigorites and serpentine pseudomorphs after several parent silicates (serpentine mineral = lizardite or lizardite + minor chrysotile) reflect the compositional differences predicted by their contrasting structural formulae. Octahedral occupancy and H<sub>2</sub>O (estimated by difference) are lower in antigorite. These data also emphasize the importance of normalizing cation proportions of serpentine analyses to the number of oxygens appropriate to their structural formula.

Solid solution of Fe, Cr, Al, Mn and Ni are significant in the serpentines studied. MgO contents of antigorites overlap completely with those of bastites and mesh-textured serpentine despite the lower total octahedral occupancy. Bastites after clinopyroxene and orthopyroxene have high Cr and Al compared to adjacent mesh pseudomorphs after olivine. This is interpreted as inheritance of the parent mineral composition due to the relative immobility of Cr and Al during low-temperature serpentinization. The distribution of iron (normalized to total octahedral cations) among adjacent serpentine pseudomorphs after olivine and pyroxene suggests a high mobility of Fe during serpentinization.

This inference is supported by the distribution of magnetite in serpentinites.

Bastites rich in trivalent cations commonly persist as unrecrystallized relics in metaserpentinities in which the low-Al mesh-textured serpentine has been converted to antigorite. Increased lizardite stability as a function of coupled Al-substitution in tetrahedral and octahedral sites has been predicted by several workers and is confirmed by the experiments of Caruso & Chernosky (1979). However, metastable persistence and a generally increased stability field for lizardite are two possible explanations for this phenomenon.

#### REFERENCES

- BEESON, M.H. & JACKSON, E.D. (1969): Chemical composition of altered chromites from the Stillwater Complex, Montana. *Amer. Mineral.* 54, 1084-1100.
- BLISS, N.W. & MACLEAN, W.H. (1975): The paragenesis of zoned chromite from central Manitoba. *Geochim. Cosmochim. Acta* 39, 973-990.
- BRINDLEY, G.W. (1963): Crystallographic aspects of some decomposition and recrystallization reactions. In *Progress in Ceramic Science* 3 (J.E. Burke, ed.), Macmillan, New York.
- & HANG, P.T. (1973): The nature of garnierites. I. Structures, chemical compositions and color characteristics. *Clays Clay Minerals* 21, 27-40.
- CARUSO, L.J. & CHERNOSKY, J.V., JR. (1979): The stability of lizardite. *Can. Mineral.* 17, 757-769.
- CHERNOSKY, J.V., JR. (1975): Aggregate refractive indices and unit cell parameters of synthetic serpentine in the system MgO-Al<sub>2</sub>O<sub>3</sub>-SiO<sub>2</sub>-H<sub>2</sub>O. *Amer. Mineral.* 60, 200-208.
- COLEMAN, R.G. (1971): Petrologic and geophysical nature of serpentinites. *Geol. Soc. Amer. Bull.* 82, 897-918.
- DIETRICH, V. & PETERS T. (1971): Regionale Verteilung der Mg-Phyllosilikate in den Serpentiniten der Oberhalbsteins. *Schweiz. Mineral. Petrog. Mitt.* 51, 329-348.
- DUNGAN, M.A. (1974): *The Origin, Emplacement and Metamorphism of the Sultan Mafic-Ultramafic Complex, Northern Cascades, Snohomish County, Washington*. Ph.D. thesis, Univ. Washington, Seattle, Wash.
- (1977): Metastability in serpentine-olivine equilibria. *Amer. Mineral.* 62, 1018-1029.
- (1979): Bastite pseudomorphs after orthopyroxene, clinopyroxene and tremolite. *Can. Mineral.* 17, 729-740.
- & VANCE, J.A. (1972): Metamorphism of ultramafic rocks from the upper Stillaguamish river area, North Cascades, Washington. *Geol. Soc. Amer. Program Abstr.* 4, 493.

- ECKSTRAND, O.R. (1975): The Dumont serpentinite: a model for control of nickeliferous opaque mineral assemblages by alteration reactions in ultramafic rocks. *Econ. Geol.* 70, 183-201.
- EVANS, B.W. & TROMMSDORFF, V. (1970): Regional metamorphism of ultramafic rocks in the central Alps: parageneses in the system CaO-MgO-SiO<sub>2</sub>-H<sub>2</sub>O. *Schweiz. Mineral. Petrog. Mitt.* 50, 481-492.
- FAUST, G.T. & FAHEY, J.J. (1962): The serpentine group minerals. *U.S. Geol. Surv. Prof. Pap.* 384A.
- FLORAN, R.J. & PAPIKE, J.J. (1975): Petrology of the low-grade rocks of the Gunflint iron-formation, Ontario-Minnesota. *Geol. Soc. Amer. Bull.* 86, 1169-1190.
- FROST, B.R. (1973): *Contact Metamorphism of the Ingalls Ultramafic Complex at Paddy-Go-Easy Pass, Central Cascades, Washington*. Ph.D. thesis, Univ. Washington, Seattle, Wash.
- (1975): Contact metamorphism of serpentinite, chloritic blackwall and rodingite at Paddy-Go-Easy Pass, Central Cascades, Washington. *J. Petrology* 16, 272-313.
- GILLERY, F.H. (1959): The X-ray study of synthetic Mg-Al serpentines and chlorites. *Amer. Mineral.* 44, 143-152.
- HOSTETLER, P.B., COLEMAN, R.G., MUMPTON, F.A. & EVANS, B.W. (1966): Brucite in alpine serpentinites. *Amer. Mineral.* 51, 75-98.
- JOHNSON, M., DUNGAN, M.A. & VANCE, J.A. (1977): Stable isotope compositions of olivine and dolomite in peridotites formed by deserpentinization, Darrington area, North Cascades, Washington. *Geochim. Cosmochim. Acta* 41, 431-435.
- KUNZE, G. (1956): Die gewellte Struktur des Antigorits: I. *Z. Krist.* 108, 82-107.
- (1958): Die gewellte Struktur des Antigorits: II. *Z. Krist.* 110, 282-320.
- (1961): Antigorit. Strukturtheoretische Grundlagen und ihre praktische Bedeutung für die weitere Serpentin-Forschung. *Fortschr. Mineral.* 39, 206-324.
- MATTHES, S. (1971): Die ultramafischen Hornfelse, insbesondere ihre Phasenpetrologie. *Forsch. Mineral.* 48, 108-127.
- ONYEAGOGCHA, A.C. (1973): *Petrology and Mineralogy of the Twin Sisters Dunite, Washington*. Ph.D. thesis, Univ. Washington, Seattle, Wash.
- PAGE, N.J. (1967): Serpentinization at Burro Mountain, California. *Contr. Mineral. Petrology* 14, 321-342.
- (1968): Chemical differences among the serpentine "polymorphs". *Amer. Mineral.* 53, 201-215.
- & COLEMAN, R.G. (1967): Serpentine mineral analyses and physical properties. *U.S. Geol. Surv. Prof. Pap.* 575-B, B103-B107.
- PETERS, T. (1968): Distribution of Mg, Fe, Al, Ca and Na in coexisting olivine, orthopyroxene and clinopyroxene in the Totalp serpentinite (Davos, Switzerland) and in the alpine metamorphosed Malenco serpentine (N. Italy). *Contr. Mineral. Petrology* 18, 65-75.
- RADOSLOVICH, E.W. (1963): The cell dimensions and symmetry of layer-lattice silicates. VI. Serpentine and kaolin morphology. *Amer. Mineral.* 48, 368-378.
- ROY, D.M. & ROY, R. (1954): An experimental study of the formation and properties of synthetic serpentines and related layer silicate minerals. *Amer. Mineral.* 39, 957-975.
- RUCKLIDGE, J.C. & PATTERSON, G.C. (1977): The role of chlorine in serpentinization. *Contr. Mineral. Petrology* 65, 39-44.
- SHIROZU, H. & MOMOI, H. (1972): Synthetic Mg-chlorite in relation to natural chlorite. *Mineral. J. (Japan)* 6, 464-476.
- SIMKIN, T. & SMITH, J.V. (1970): Minor element distribution in olivine. *J. Geol.* 78, 304-325.
- TROMMSDORFF, V. & EVANS, B.W. (1972): Progressive metamorphism of antigorite schist in the Bergell tonalite aureole (Italy). *Amer. J. Sci.* 272, 423-437.
- ULMER, G.C. (1974): Alteration of chromite during serpentinization in the Pennsylvania-Maryland district. *Amer. Mineral.* 59, 1236-1241.
- VANCE, J.A. (1972): Mid-Tertiary tectonic emplacement of metamorphic peridotites in the Darrington area, Cascade Mountains, Washington. *Geol. Soc. Amer. Program Abstr.* 4, 253.
- & DUNGAN, M.A. (1977): Formation of peridotites by deserpentinization in the Darrington and Sultan areas, Cascade Mountains, Washington. *Geol. Soc. Amer. Bull.* 88, 1497-1508.
- , —, BLANCHARD, D.P. & RHODES, J.M. (1980): Tectonic setting and trace element geochemistry of Mesozoic ophiolitic rocks in western Washington. *Amer. J. Sci.* 280A, 359-388.
- WHITTAKER, E.J.W. & WICKS, F.J. (1970): Chemical differences among the serpentine "polymorphs": a discussion. *Amer. Mineral.* 55, 1025-1047.
- & ZUSSMAN, J. (1956): The characterization of serpentine minerals by X-ray diffraction. *Mineral. Mag.* 31, 107-126.
- WICKS, F.J. (1969): *X-ray and Optical Studies on Serpentine Minerals*. D.Phil. thesis, Oxford University, Oxford, England.
- & WHITTAKER, E.J.W. (1975): A reappraisal of the structures of the serpentine minerals. *Can. Mineral.* 13, 227-243.
- & — (1977): Serpentine textures and serpentinization. *Can. Mineral.* 15, 459-488.
- , — & ZUSSMAN, J. (1977): An idealized model for serpentine textures after olivine. *Can. Mineral.* 15, 446-458.
- & ZUSSMAN, J. (1975): Microbeam X-ray diffraction patterns of the serpentine minerals. *Can. Mineral.* 13, 244-258.
- ZUSSMAN, J., BRINDLEY, G.W. & COMER, J.J. (1957): Electron diffraction studies of serpentine minerals. *Amer. Mineral.* 42, 133-153.